J Pharmacokinet Pharmacodyn (2015) 42:163–177
DOI 10.1007/s10928-015-9408-2

ORIGINAL PAPER

Population pharmacokinetic and pharmacodynamic model of propofol externally validated in children

Byung-Moon Choi · Hyun-Gu Lee · Hyo-Jin Byon · Soo-Han Lee · Eun-Kyung Lee · Hee-Soo Kim · Gyu-Jeong Noh

Received: 24 May 2014 / Accepted: 13 February 2015 / Published online: 28 February 2015

Abstract There have been no pharmacokinetic parameters and blood–brain equilibration rate constant (k_{e0}) of propofol obtained in a single population of children, by which propofol can be administered using a target effect-site concentration controlled infusion. Thirty-nine, American Society of Anesthesiologists Physical Status 1–2 children aged 2–12 years were given an intravenous bolus of propofol (3 mg kg^{-1}), followed by infusion (200 μg kg^{-1} min^{-1}). Arterial drug concentrations and bispectral index (BIS) values were measured. Population pharmacokinetic and pharmacodynamic analysis was performed using nonlinear mixed effects modeling. External model validation was performed in a separate population of children. A two-compartment model and a sigmoid E_{max} model directly linked by an effect compartment well described the time courses of propofol concentration and BIS. The estimates of parameters were: V_1 (L) = 1.69, V_2 (L) = 27.2 + 0.929 × (weight − 25), Cl (L min^{-1}) = 0.893 × (weight/23.6)$^{0.966}$, Q (L min^{-1}) = 1.3; E_0 = 76.9; E_{max} = 35.4, Ce_{50} (μg mL^{-1}) = 3.47 − (0.095 × age) − (1.63 × mean infusion rate of remifentanil in μg kg^{-1} min^{-1}); γ = 2.1; and k_{e0} (min^{-1}) = 0.371. Pooled biases (95 % CI) of the target effect-site concentration controlled infusion system of propofol was −20.2 % (−23.3 to −18.1 %) and pooled inaccuracy was 30.4 % (28.6–32.7 %). Pooled biases of BIS prediction was −6.8 % (−9.1 to −4.1 %) and pooled inaccuracies was 19.1 % (17.5–20.9 %).The altered weight-based dose requirements of propofol are well described pharmacokinetically, and pharmacodynamically. Predictive performances of the TCI system in this study were clinically acceptable.

Keywords Propofol · Pharmacokinetics · Pharmacodynamics

Byung-Moon Choi and Hyun-Gu Lee contributed equally to this work as first authors and Hee-Soo Kim and Gyu-Jeong Noh also contributed equally to this work as corresponding authors.

Electronic supplementary material The online version of this article (doi:10.1007/s10928-015-9408-2) contains supplementary material, which is available to authorized users.

B.-M. Choi · G.-J. Noh (✉)
Department of Anesthesiology and Pain Medicine, Asan Medical Center, University of Ulsan College of Medicine, 388-1 Pungnap 2-dong, Songpa-gu, Seoul 138-736, Korea
e-mail: nohgj@amc.seoul.kr

H.-G. Lee
University of Ulsan College of Medicine, Seoul, Korea

H.-J. Byon
Department of Anesthesiology and Pain Medicine, Yonsei University College of Medicine, Seoul, Korea

S.-H. Lee · G.-J. Noh
Department of Clinical Pharmacology and Therapeutics, Asan Medical Center, University of Ulsan College of Medicine, Seoul, Korea

E.-K. Lee
Department of Statistics, Ewha Womans University, Seoul, Korea

H.-S. Kim (✉)
Department of Anesthesiology and Pain Medicine, Seoul National University Hospital, Seoul National University College of Medicine, 101 Daehak-ro, Jongno-gu, Seoul 110-744, Korea
e-mail: dami0605@snu.ac.kr

Introduction

Although total intravenous anaesthesia using target-controlled infusion (TCI) of propofol affords many advantages, plasma propofol concentration is poorly predicted and highly variable between individuals, when employed in pediatric patients [1]. The propofol induction and maintenance dose requirements are higher in younger children than in older children or adults [2]. The typical pharmacokinetic and pharmacodynamic characteristics of propofol in children, such as a greater central volume of distribution and elevated systemic clearance [3, 4], and possibly also a lower potency may account for this [5, 6]. Although the cited studies identified that children showed an elevated pharmacodynamic sensitivity to propofol, the pharmacodynamic parameters of propofol remain controversial and no pharmacokinetic/pharmacodynamic model is currently available for use in pediatric anaesthesia. For example, it is unclear whether the elevation in propofol dose required by children is attributable to age-related pharmacokinetic characteristics, primarily determined by body composition [7, 8], or to variation in drug potency. To explore these questions, we considered that a pharmacokinetic/pharmacodynamic study in a single population of children was desirable. Also, external validation of these models developed should be required to infuse propofol with target-controlled infusion in children.

The electroencephalographic bispectral index (BIS) monitors the depth of hypnosis in children [9]. In general, opioids per se have no influence on the BIS [10]. However, when combined with propofol, remifentanil exhibits an additive effect on the median power frequency of processed electroencephalograms [11] or synergistic effects on both the BIS [12] and various clinical endpoints [13]. When propofol and remifentanil are co-administered during total intravenous anaesthesia, the effect of remifentanil on the pharmacodynamic response to propofol should be considered.

This study aimed to characterize pharmacokinetics and pharmacodynamics of propofol in children ranging in age from 2 to 12 years during total intravenous anaesthesia and to evaluate predictive performance of these models in a separate population of children.

Methods

Patient population

All patients underwent elective urologic or orthopedic surgery under total intravenous anaesthesia with propofol and remifentanil. With the approval from the Institutional Review Board of Seoul National University Hospital (Seoul, Korea), and all parents provided informed consents before children were enrolled in this study. Any patient who had medical problems, significantly abnormal laboratory findings, pubertal staging in terms of clinical observation of external secondary sexual characteristics, or who received preoperative drugs that altered anesthetic depth or electroencephalographic features was excluded.

Study procedure

Thirty-nine patients were enrolled in the pharmacokinetic and pharmacodynamic model building. All patients fasted (for 6 h for patients aged 24–36 months; for 8 h for those aged more than 36 months) prior to surgery. Premedication including midazolam (0.1 mg kg^{-1}, up to 5 mg) and atropine (0.02 mg kg^{-1}, up to 0.5 mg) was intravenously administered in the reception area. Once in the operating room, electrocardiography, pulse oximetry, invasive blood pressure measurement (Solar 8000M, GE Medical Systems Information Technologies, Inc., Milwaukee, WI), and BIS (Aspect 2000, Aspect Medical Systems, Inc., Newton, MA) were monitored in all patients. All data were recorded both at baseline and continuously until the end of anaesthesia. During pre-oxygenation using a face mask with 100 % oxygen, twenty milligrams of lidocaine were intravenously administered prior to propofol injection. Subsequently, intravenous boluses of propofol (2 % Fresofol®, Fresenius Kabi Korea Ltd., Seoul, Korea) 3 mg kg^{-1} and remifentanil (Ultiva®, GlaxoSmithKline Korea, Seoul, Korea) 1 μg kg^{-1} were given. When patients became unconscious, propofol was infused at 200 μg kg^{-1} min^{-1} and remifentanil was administered at 0.2 μg kg^{-1} min^{-1}. During maintenance of anaesthesia, propofol and remifentanil were infused to maintain the BIS value at under 60, and the systolic blood pressure and heart rate at 120 % or less of the preoperative stable values measured in the ward. The trachea was intubated after administering rocuronium 0.6 mg kg^{-1} intravenously. The lungs were then ventilated with 65 % N_2O in O_2, with the end-tidal carbon dioxide partial pressure maintained between 30 and 40 mmHg.

Blood sampling and assays

One-milliliter of arterial blood was sampled into ethylenediamine-tetra-acetic acid (EDTA) immediately before induction; and at 2, 5, 10, 15 and 30 min after the first intravenous bolus of propofol. Samples were also collected at 0, 2, 5, 10, 30, 60, and 120 min after propofol was discontinued.

All samples were centrifuged for 10 min at 252×*g*, and stored at −70 °C until assay. Plasma concentrations of propofol were measured by high-performance liquid chromatography using a Capcell Pak C18 UG120 column

(Shiseido Fine Chemicals, Tokyo, Japan) and a mixture of acetonitrile, methanol and trifluoroacetic acid (56:44:0.1, v/v/v) as a mobile phase. The column effluent was monitored using a fluorometric detector with the excitation and emission wavelengths set at 276 nm and 310 nm. The lower limit of propofol quantification was 100 ng mL^{-1}. The calibration curve was linear over the range of 100–10,000 ng mL^{-1}, with the coefficients of determination (R^2) greater than 0.997 for all instances. The intra-assay precision value was 1.7–3.7 % and inter-assay was 2.0–5.3 %. The intra-assay accuracy value was 88.4–100.6 % of nominal value and inter-assay was 87.7–96.4 %.

Population pharmacokinetic and pharmacodynamics analysis

The procedures of NONMEM VII level 2 (ICON Development Solutions, Ellicott City, MD) employed in pharmacokinetic and pharmacodynamic modeling were the ADVAN 6 subroutines and first-order conditional estimation with interaction. Inter-individual random variabilities of pharmacokinetic and pharmacodynamic parameters were modeled using a log-normal or additive model, as appropriate. Diagonal matrices were estimated for the various distributions of η, where η represented inter-individual random variability with a mean of zero and a variance of ω^2. Additive, constant coefficient of variation, and combined additive and constant coefficient of variation residual error models were evaluated during the model building process. NONMEM computed the minimum value of the objective function, a statistic equivalent to the −2 log likelihood of the model. An α level of 0.05, which corresponds to a reduction in the objective function value of 3.84 (Chi squared distribution, degree of freedom: 1, $p < 0.05$), was used to discriminate between hierarchical models [14]. In addition to obtaining minimal objective function values, improvements in diagnostic goodness-of-fit plots were used to evaluate different models. R software (version 2.13.1; R Foundation for Statistical Computing, Vienna, Austria) was employed to construct graphical model diagnostics. Covariate model-building was performed using manual covariate selection.

One-, two-, and three-compartment models with linear pharmacokinetics were tested. Covariates analyzed were age, sex, weight, height, body surface area [15], lean body mass [16], body mass index, body fat level [17], fat-free mass [18], estimated glomerular filtration rate [19], blood protein concentration, blood albumin level and the mean infusion rate of remifentanil throughout the operative period (bolus and infusion doses divided by the elapsed time from the first bolus to the end of infusion) and bolus dose of midazolam.

The effect of body weight on all of the volume and clearance parameters was predicted on the basis of allometric scaling or linear relationship as follows [20, 21]:

$$P_i = \theta_p \left(\frac{BW_i}{mean\ of\ BW_i} \right)^{\theta} \exp(\eta_i)\ or\ P_i = \left(\theta_p + (BW_i - mean\ of\ BW_i) \times \theta \right) \exp(\eta_i) \quad (1)$$

where P_i denotes the individual value, θ_p means the population estimates, BW_i is the individual body weight.

A sequential modeling approach with posthoc pharmacokinetic estimates was used to derive the population pharmacodynamic parameters. Dissociation between the concentration of propofol and effect (BIS) was linked with an effect compartment. The relationship between the effect-site concentration of propofol and BIS was evaluated using a sigmoid E_{max} model:

$$Effect = E_0 + (E_{\max} - E_0) \frac{Ce^{\gamma}}{Ce_{50}^{\gamma} + Ce^{\gamma}} \quad (2)$$

where *Effect* is the BIS value, E_0 is the baseline BIS value when no drug was present, E_{max} is the maximum possible drug effect on the BIS, Ce is the calculated effect-site concentration of propofol, Ce_{50} is the effect-site concentration associated with 50 % of the maximal drug effect on BIS, and γ is the steepness of the effect-site concentration versus BIS relationship.

Also, the time course of BIS was directly linked to the effect compartment concentration through the E_{max} model to describe drug interaction with midazolam:

$$Effect = E_0 \left(1 - E_{\max} \frac{\left(\frac{C_e}{C_{e50}} + MID \right)^{\gamma}}{1 + \left(\frac{C_e}{C_{e50}} + MID \right)^{\gamma}} \right) \quad (3)$$

where E_{max} is the maximal effect fixed to 1 and C_{e50} is the concentration for the 50 % decrease in the BIS score caused by propofol. The parameter MID = $C_{Mid}/C_{e50,Mid}$ equals to the ratio of midazolam concentration and $C_{e50,Mid}$ value of midazolam. Thus, Ce/C_{e50} + MID denotes the virtual effect concentration, which is defined as the sum of the normalized effect-site concentrations of propofol and midazolam assuming the additive interaction of these drugs [22]. In addition, a two-compartment effect site model was applied to describe the time course of BIS. The model well described change of BIS after different rates of propofol infusion [23]. The covariates analyzed in pharmacodynamic modeling were the same as those described above.

Model diagnosis and validation

The level of significance of a covariate was additionally assessed using a randomization test which randomly permutes the covariate in the original dataset (fit4NM 3.7.9,

Eun-Kyung Lee and Gyu-Jeong Noh, http://www.fit4nm.org/download, last accessed: Oct 17, 2011). The differences in objective function values between reference (without the covariate tested) and covariate (containing the covariate tested) models fitted to the permuted datasets were sorted in ascending order. The value corresponding to the 5th percentile was set as the δ value. If a change in objective function values between reference and covariate models fitted to an original dataset was greater than the δ value, this was considered to be good evidence that the covariate effect was statistically significant [24].

Non-parametric bootstrap analysis served to internally validate models (fit4NM 3.7.9) [25]. Briefly, 2,000 bootstrap replicates were generated by random sampling from the original dataset, with replacement. Parameter estimates were compared with median parameter values and the 2.5–97.5 percentiles of the nonparametric bootstrap replicates. Predictive checks were performed by simulating 2,000 iterations and comparing the 90 % prediction intervals to the original data (fit4NM 3.7.9) [26]. Prediction correction for dependent variable, Y_{ij}, with lower bound, lb_{ij} [27]:

$$pcY_{ij} = lb_{ij} + (Y_{ij} - lb_{ij}) \cdot \frac{\tilde{PRED}_{bin} - lb_{ij}}{PRED_{ij} - lb_{ij}} \quad (4)$$

where Y_{ij} means observation or prediction for the ith individual and jth time point, pcY_{ij} is prediction-corrected observation or prediction, $PRED_{ij}$ stands for typical population prediction for the ith individual and jth time point, and $PRED_{bin}$ is median of typical population predictions for the specific bin of independent variables.

External validation

One hundred fifty-five patients were enrolled in the predictive performance of pharmacokinetic and pharmacodynamic models (Table 1). Propofol was infused with TCI software (Asan pump, version 2.1.3; Bionet Co. Ltd., Seoul, Korea, http://www.fit4nm.org/download, last accessed: Aug 27, 2012) with BIS monitoring. Pharmacokinetic parameters and blood–brain equilibration rate constant (k_{e0}) in Tables 2 and 3 were programmed into the Asan pump. Premedication including midazolam (0.1 mg kg^{-1}, maximum of 5 mg) and atropine (0.02 mg kg^{-1}, maximum of 0.5 mg) was intravenously administered in the reception area. Propofol was administered by stepwise increase and decrease in the effect-site concentration and the order of target concentrations was 4, 5, 3 and 2 μg mL^{-1}, with each concentration being maintained for at least 10 min. Arterial blood (1 mL) was sampled at least 10 min after every change in a target concentration of propofol.

As described in the earlier study [28], four parameters including inaccuracy, divergence, bias and wobble, were used to evaluate the performance of a TCI system.

First, for each blood sample and BIS value, the performance error (PE) of the *i*th individual was calculated as:

$$PE_{ij} = \frac{measured_{ij} - predicted_{ij}}{predicted_{ij}} \quad (5)$$

where $predicted_{ij}$ is the *j*th prediction of the effect-site propofol concentration or BIS value in the *i*th individual, whereas $measured_{ij}$ is the measurement of the plasma propofol concentration or BIS value. The predicted BIS value in each point was calculated from the sigmoid E_{max} model using pharmacodynamic parameters in Table 3.

The inaccuracy, for the *i*th patient, was reflected by calculating the median absolute performance error ($MDAPE_i$):

$$MDAPE_i = median\{|PE_{ij}|,\ j = 1, \ldots N_i\} \quad (6)$$

where N_i is the number of PE in the *i*th individual.

Divergence was calculated, for the *i*th patient, as the slope acquired from the linear regression of that individual's the $|PE_{ij}|$s against time:

Table 1 Characteristics of patients for model building and external validation of pharmacokinetic and pharmacodynamic models ($n = 155$)

	Model building ($n = 39$)	External validation		
		Pharmacokinetic model ($n = 155$)	Pharmacodynamic models ($n = 155$)	
			Intermediate model ($n = 78$)	Final model ($n = 77$)
ASA PS 1/2	35/4	132/23	67/11	65/12
Sex (M/F)	35/4	78/77	40/38	38/39
Age (years)	5 (2–12)	6 (0.2–12)	6 (0.2–12)	6 (0.2–12)
Weight (kg)	21 (11.9–39.1)	21 (5.2–65)	22.5 (5.2–65)	21.0 (6.2–61)
Height (cm)	115.7 ± 17.1	113.4 ± 26.2	113.6 ± 26.6	113.3 ± 26.1

Data are presented as counts or means ± SDs (ranges) or median (ranges) as appropriate. ASA PS, American Society of Anesthesiologists physical status. Patient characteristics enrolled in the external validation of pharmacodynamic models were compared using the two-sample *t* test, Mann–Whitney rank-sum test, or χ^2 test as appropriate. No significant differences were found between any of the observations

Table 2 Population pharmacokinetic parameter estimates, inter-individual variability (IIV) and median parameter values (2.5–97.5 %) of the nonparametric bootstrap (BS) replicates of the final pharmacokinetic model of propofol in children

Model	Parameters	Definition	Estimates (RSE, %)	CV (%)	BS median	BS 95 % CI
Basic	V_1 (L)	Central volume of distribution	2.12 (9.9)	47.8	–	–
	V_2 (L)	Peripheral volume of distribution	24.4 (6.7)	37.0	–	–
	Cl (L min^{-1})	Metabolic clearance	0.86 (14.0)	45.6	–	–
	Q (L min^{-1})	Inter-compartmental clearance	1.32 (29.4)	92.5	–	–
	σ (%)	Standard deviation of RRV	5.2 (4.9)	–	–	–
Final	V_1 (L)	Central volume of distribution	1.69 (33.2)		1.77	0.66–2.82
	V_2 (L)	Peripheral volume of distribution	θ_1: 27.2 (7.1)		27.2	22.3–32.0
	$= \theta_1 + \theta_2 \times (\mathrm{WT} - 25)$		θ_2: 0.93 (21.0)		0.93	0.35–1.51
	Cl (L min^{-1})	Metabolic clearance	θ_3: 0.89 (12.2)		0.89	0.8–0.98
	$= \theta_3 \times (\mathrm{WT}/23.6)^{\theta_4}$		θ_4: 0.97 (31.5)		0.94	0.68–1.18
	Q (L min^{-1})	Inter-compartmental clearance	1.3 (33.8)		1.32	0.94–1.74
	σ (%)	Standard deviation of RRV	5.2 (6.7)	–	5.1	4.5–5.8
	ω^2 for V_1	IIV for V_1	0.763 (93.4)	87.4	0.649	0.001–2.26
	ω^2 for V_2	IIV for V_2	0.035 (94.2)	18.6	0.032	0.001–0.146
	ω^2 for Cl	IIV for Cl	0.095 (63.5)	30.9	0.087	0.033–0.196
	ω^2 for Q	IIV for Q	0.824 (59.2)	90.8	0.782	0.255–1.36

A log-normal distribution of IIV was assumed. Residual random variability (RRV) was modeled using a constant coefficient of variation (CV) model. Nonparametric BS analysis was repeated 2000 times. The eta-shrinkage for V_1, V_2, Cl, Q were 36.4, 42.9, 2.8 and 11.2 %, respectively

RSE relative standard error = SE/mean × 100 (%), *CI* confidence interval, *WT* body weight (kg)

$$Divergence_i\,(\%\,h^{-1}) = 60 \times \frac{\sum_{j=1}^{N_i}|PE_{ij}| \times t_{ij} - \left(\sum_{j=1}^{N_i}|PE_{ij}|\right) \times \left(\sum_{j=1}^{N_i} t_{ij}\right)/N_i}{\sum_{j=1}^{N_i}(t_{ij})^2 - \left(\sum_{j=1}^{N_i} t_{ij}\right)^2/N_i} \quad (7)$$

where t_{ij} is the time at which the corresponding PE_{ij} was determined.

The third performance measure, a measure of bias, for the *i*th patient was reflected by calculating the median performance error ($MDPE_i$):

$$MDPE_i = median\{PE_{ij},\ j = 1, \ldots N_i\} \quad (8)$$

The fourth performance measure, $Wobble_i$, for the *i*th individual was simply a measure of the variability of the PE_{ij} in the *i*th individual:

$$Wobble_i = \text{median absolute deviation of } \{PE_{ij},\ j = 1, \ldots N_i\} \text{ from } MDPE_i \quad (9)$$

Population estimates of these performance measures was calculated by a pooled data approach (fit4NM 3.7.9) [28].

Simulations

Deterministic simulations, considering neither inter-individual nor intra-individual random variability, were performed using Asan Pump software. The time courses of propofol concentrations in the plasma and effect-site, and BIS, after an intravenous bolus of 3 mg kg^{-1}, and after zero-order infusion at the rate of 200 μg kg^{-1} min^{-1} for 60 min, were simulated in hypothetical children weighing 10 and 40 kg. Context-sensitive decrement times (50 and 80 %) over the durations of target plasma concentration-controlled infusion were calculated.

Statistics

Prediction probability (P_K), a parameter showing nonparametric correlation known as a measure of association, was calculated using Somers′ d formula (fit4NM 3.7.9), which was then transformed from the −1 to 1 scale of Somers′ d to the 0 to 1 scale of P_K as $P_K = 1 - (1 - |\text{Somers' d}|) \times 2^{-1}$ [29]. Observed BIS values and effect-site concentrations of propofol predicted by pharmacodynamic models were set as the observation and prediction values. Datasets used were those for model building and external validation. The SE of each P_K was calculated as (SE of Somers′ d) × 2^{-1}.

Results

Thirty-nine patients, aged 2–12 years, were enrolled for model building. The duration of operation was 155 ± 80 min. The amount of propofol administered by intravenous bolus during induction was 71 ± 25 mg, and that by continuous infusion

Table 3 Population parameter estimates, inter-individual variability (IIV), and median parameter values (2.5–97.5 %) of the non-parametric bootstrap (BS) replicates of the pharmacodynamic models of propofol in children

Model	Parameter	Definition	Estimate (RSE, %)	CV (%)	BS median	BS 95 % CI
Basic	E_0	Baseline BIS value before propofol administration	76.9 (4.16)			
	E_{max}	Minimum possible BIS value	35.6 (11.43)	15.33		
	C_{e50} (μg mL^{-1})	Ce at 50 % of the maximal propofol effect on BIS	2.61 (13.03)	7.75		
	γ	Steepness of the Ce versus BIS relationship	3.05 (38.36)			
	k_{e0} (min^{-1})	Blood brain equilibration rate constant	0.557 (20.47)	20.01		
	σ	Standard deviation of RRV	8.5 (14.39)			
Intermediate	E_0	Baseline BIS value before propofol administration	76.9 (4.15)		77.8	72.1–82.9
	E_{max}	Minimum possible BIS value	35.4 (11.41)		35.2	20–41.4
	C_{e50} (μg mL^{-1}) $= \theta_1 - \theta_2 \times$ AGE	Ce at 50 % of the maximal propofol effect on BIS	θ_1: 3.78 (11.93)		3.66	2.26–5
			θ_2: 0.183 (29.07)		0.167	0.011–0.32
	γ	Steepness of the Ce versus BIS relationship	3.02 (38.08)		2.97	1.46–5.56
	k_{e0} (min^{-1})	Blood brain equilibration rate constant	0.557 (18.85)		0.55	0.31–0.78
	σ	Standard deviation of RRV	8.5 (14.5)		8.4	7.3–9.7
	ω^2 for E_{max}	IIV for E_{max}	0.060 (44.9)	24.43		
	ω^2 for C_{e50}	IIV for C_{e50}	0.263 (73.8)	51.19		
	ω^2 for k_{e0}	IIV for k_{e0}	1.26 (45.5)	112.3		
Final	E_0	Baseline BIS value before propofol administration	79.9 (2.34)		81.3	78.2–85.2
	E_{max}	Minimum possible BIS value	30.6 (7.94)		30.7	20.0–37.9
	C_{e50} (μg mL^{-1}) $= \theta_3 - \theta_4 \times$ AGE $- \theta_5 \times$ REMI	Ce at 50 % of the maximal propofol effect on BIS	θ_3: 3.65 (11.2)		3.54	2.80–5.0
			θ_4: 0.102 (27.75)		0.1	0.06–0.20
			θ_5: 1.72 (19.13)		1.66	0.05–2.5
	γ	Steepness of the Ce versus BIS relationship	2.11 (9.91)		2.10	1.54–3.0
	k_{e0} (min^{-1})	Blood brain equilibration rate constant	0.372 (38.34)		0.38	0.3–0.6
	σ^2	Standard deviation of RRV	8.4 (1.65)	–	8.3	7.0–9.1
	ω^2 for E_{max}	IIV for E_{max}	0.047 (57.8)	21.07		
	ω^2 for C_{e50}	IIV for C_{e50}	0.106 (44.2)	37.15		
	ω^2 for k_{e0}	IIV for k_{e0}	1.27 (61.8)	128.1		

IIV of E_0 was modeled using an additive error model. Log-normal distribution was assumed for E_{max}, C_{e50}, and k_{e0}. Residual random variability (RRV) was modeled using an additive error model. Nonparametric bootstrap analysis was repeated 2,000 times. The eta-shrinkage of the intermediate model for E_{max}, C_{e50}, k_{e0} were 15.7, 7.8, and 20.4 %, respectively. The eta-shrinkage of the final model for E_{max}, C_{e50}, k_{e0} were 15.7, 7.8, and 20.4 %, respectively

C_e, calculated effect-site concentration of propofol; AGE, age (year); REMI, mean infusion rate of remifentanil throughout the operative period (bolus and infusion doses divided by the elapsed time from the first bolus to the end of infusion, μg kg^{-1} min^{-1}); RSE, relative standard error = SE/mean × 100 (%)

during maintenance was 724 ± 432 mg. The mean infusion rate of propofol during maintenance (infusion dose/infusion duration) was 200 ± 2 μg kg^{-1} min^{-1}. Three children (age and weight: 3 years and 17 kg, 4 years and 22 kg, 9 years and 28 kg) were given an additional intravenous bolus of propofol during maintenance (50, 20, and 20 mg). In one female patient aged 4 years, the infusion rate of propofol was reduced to 156 μg kg^{-1} min^{-1} from the midpoint of anaesthesia maintenance. Otherwise, propofol was administered as described above. The amount of remifentanil administered by intravenous bolus during induction was 24 ± 8 μg and that by continuous infusion during maintenance was 749 ± 402 μg. The mean infusion rate of remifentanil was 0.24 ± 0.17 μg kg^{-1} min^{-1} (range 0.203–1.214 μg kg^{-1} min^{-1}). Bolus

dose of midazolam administered prior to the administrations of propofol and remifentanil was 2.4 ± 0.8 mg (range 1.2–3.9 mg). The time courses of observed plasma concentrations of propofol and BIS in children for model building are shown in Fig. 1.

Pharmacokinetics

A total of 405 (7–15 per a child) plasma concentration measurements were available to characterize pharmacokinetics. Numbers (%) of samples within 5 after a bolus dose of propofol was 30 (7.5 %) and those within 10 min was 77 (19 %). Parameter estimates of competing basic and covariate pharmacokinetic models of propofol in children were evaluated. Pharmacokinetics of propofol in children was best described by a two-compartment model with linear pharmacokinetics. No significant covariates were found for the central volume of distribution of propofol. Thus, the central volume of distribution was fixed in children, irrespective of age, sex or body size parameters. However, the peripheral volume of distribution was proportional to body weight in kg (Eq. 10), resulting in an improvement in OFV (16, $p < 0.001$, degree of freedom: 1), compared with the basic model (number of model parameters: 9)

$$V_2 = 27.2 + 0.93 \times (\text{body weight} - 25). \quad (10)$$

Body weight was also a significant covariate for metabolic clearance of propofol, leading to a further improvement in the objective function value (28, $p < 0.001$, degree of freedom: 1) compared with that of a pharmacokinetic model which included body weight as a covariate for the peripheral volume of distribution only. Equation 11 describes the relationship between body weight and the metabolic clearance of propofol in children

$$\text{Cl} = 0.89 \times (\text{body weight}/23.6)^{0.97}. \quad (11)$$

The δ value between the basic and covariate (body weight on V_2) models in a randomization test was 2.486. The difference in the OFVs of the two models was 16 when fitted to the original dataset. The δ value between the covariate (body weight on V_2) and final pharmacokinetic (body weight on V_2 and Cl) models was 10.652. The difference in objective function values between these two models, fitted to the original dataset, was 28. This afforded sufficient evidence to conclude that the effect of body

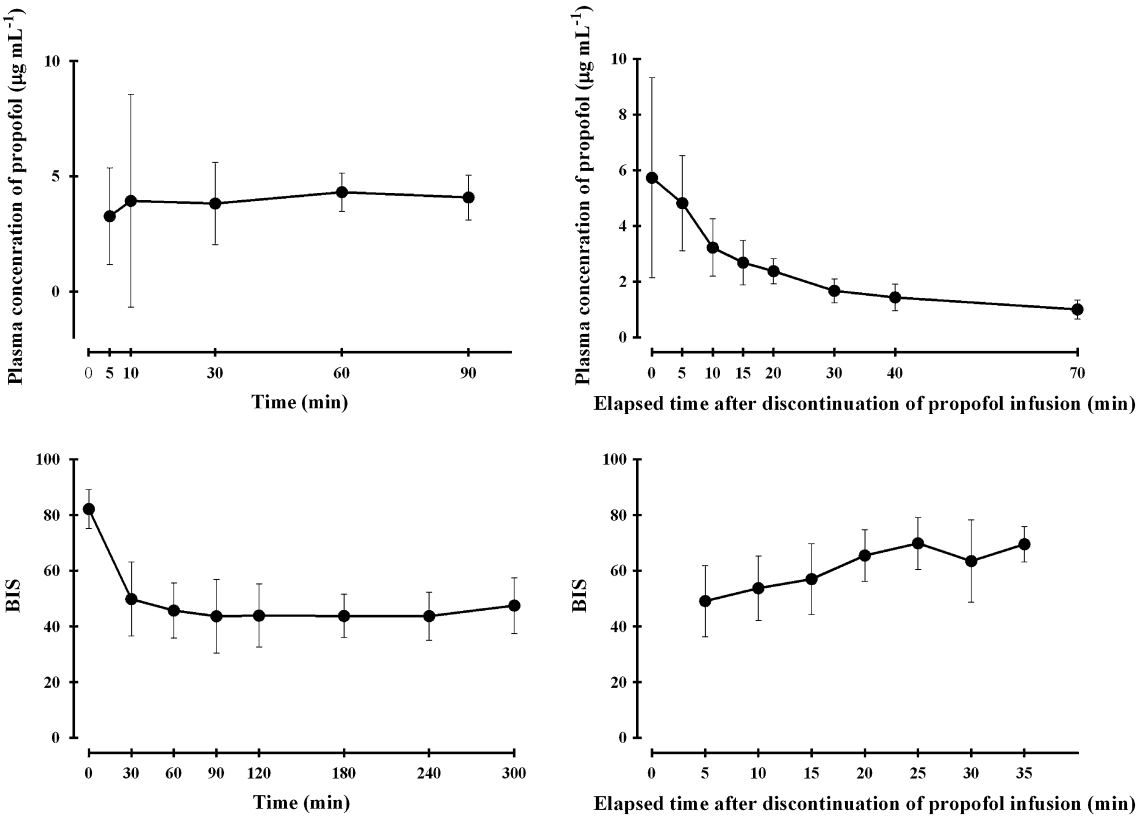

Fig. 1 Observed plasma concentrations of propofol (*upper*) and bispectral index (BIS, *lower*) values over time in 39 children, receiving an intravenous bolus of propofol 3 mg kg^{-1} followed by continuous infusion at variable rates during operation. These figures were presented with mean and error bar data, which were used for model building

weight on both V_2 and Cl was statistically significant. Relation of individual Bayesian predicted values of clearance *versus* weight was shown in Fig. 2, upper panel.

Table 2 shows population pharmacokinetic parameter estimates and the results of nonparametric bootstrap replicates of the final pharmacokinetic model. Overall, the bootstrap medians were close to the population parameter estimates and the 95 % confidence intervals of these parameters were relatively small, indicating that the parameter estimates of the final pharmacokinetic model of propofol in children were accurate and precise. Basic goodness-of-fit plots are shown in Fig. 3, left panels.

Pharmacodynamics

A total of 1159 BIS values were used to determine pharmacodynamic characteristics. Comparison between sigmoid Emax, interaction and two-compartment effect site models was shown in Supplemental Material (Table S3).

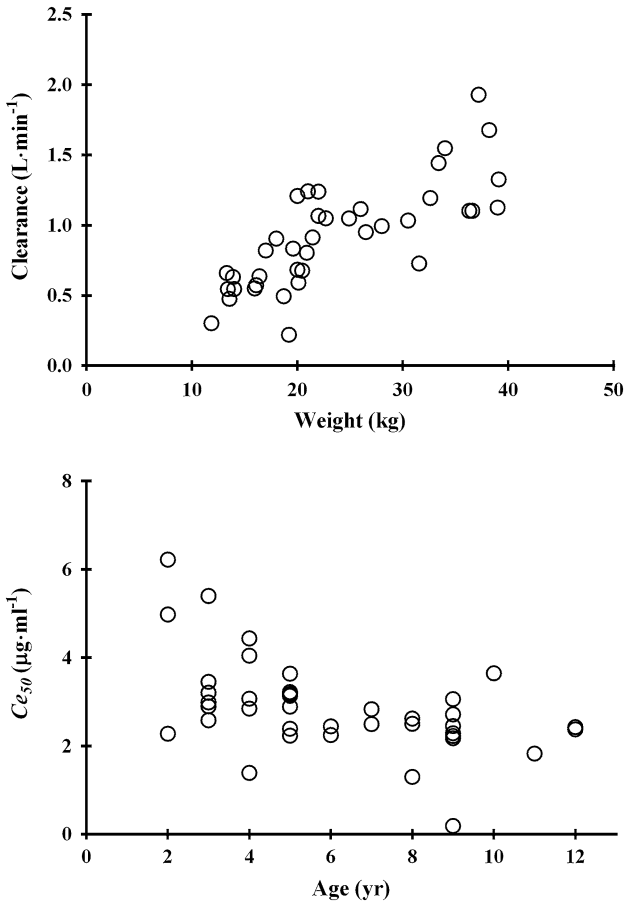

Fig. 2 Relation of individual Bayesian predicted values of clearance versus weight (*upper panel*), and Ce_{50} versus age, derived from results of final pharmacokinetic and pharmacodynamic models. As weight increases, clearance decreases. As age increases, Ce_{50} decreases

An inhibitory sigmoid Emax model well described the time course of observed BIS values. Age was a significant covariate of the Ce_{50} of propofol (Eq. 12, from an intermediate model), which resulted in improvement of the OFV (7.131, $p < 0.05$, degree of freedom: 1) in comparison with the basic model (number of model parameters: 9).

$$Ce_{50} = 3.78 - 0.183 \times \text{age}. \quad (12)$$

The typical value of Ce_{50} of propofol in the intermediate model decreased by 53.6 % as age increased from 2 to 12 years.

The addition of mean infusion rate of remifentanil to the Ce_{50} (Eq. 13, from the final model) further decreased the OFV by 48.038 ($p < 0.001$, degree of freedom: 1), compared with that of the intermediate model

$$Ce_{50} = 3.47 - 0.095 \times \text{age} - 1.63 \times \text{mean infusion rate of remifentanil}. \quad (13)$$

The typical value of Ce_{50} of propofol in the final model decreased by 29.0 % as age increased from 2 to 12 years (the mean infusion rate of remifentanil was set at 0 μg kg^{-1} min^{-1}), while decreased by 74.3 % with increasing the mean infusion rate of remifentanil from 0.2 to 1.2 μg kg^{-1} min^{-1} (age was set at 10 years). Relation of individual Bayesian predicted values of Ce_{50} versus age was shown in Fig. 2, lower panel.

The δ values between the basic and intermediate models, and between the intermediate and final models were 5.388 and 32.771. The differences in the each OFV between both models, fitted to the original dataset, were 7 and 48, suggesting that the effect of age on Ce_{50} in the intermediate model, and both age and mean infusion rate of remifentanil on Ce_{50} in the final model were statistically significant. Population pharmacodynamic parameter estimates, inter-individual variability, and median parameter values (2.5–97.5 %) of the nonparametric bootstrap replicates of the pharmacodynamic models (intermediate and final) are shown in Table 3. The biases between the bootstrap medians and population parameter estimates, and 95 % confidence intervals of parameters were also small enough to indicate that the parameter estimates of both models were reliable. Basic goodness-of-fit plots are presented in Fig. 3, right panels. The intermediate model also showed good performance and predictability close to those of the final model (the plots of basic goodness-of-fit and predictive checks are not shown), as revealed by the fact that the percentage of data distributed outside the 90 % prediction interval was 5.7 %. Prediction probability (SE, 95 % confidence interval) of propofol effect-site concentration was 0.6845 (0.0099, 0.6650–0.7039) for intermediate pharmacodynamic model and that was 0.6836 (0.0099, 0.6643–0.7029) for final pharmacodynamic model.

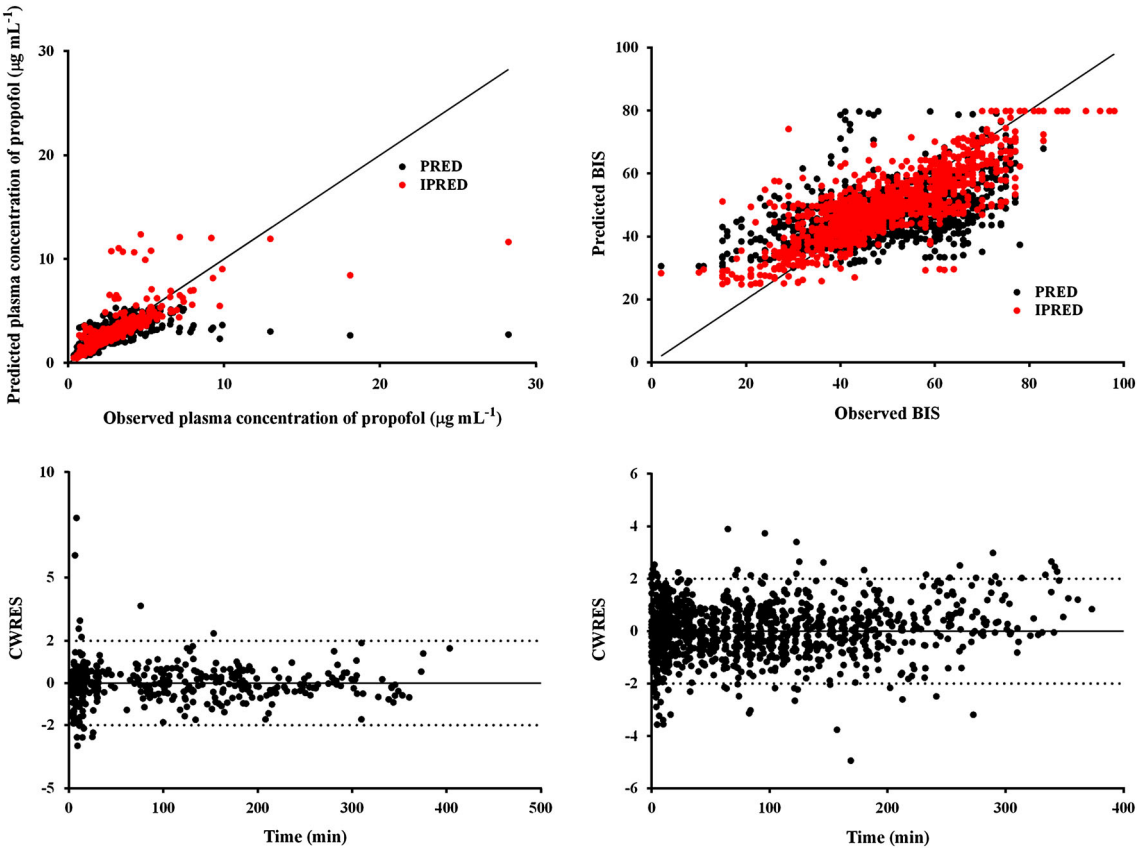

Fig. 3 Goodness-of-fit plots of the final pharmacokinetic (*left panels*) and pharmacodynamic (*right panels*) models of propofol in children ($n = 39$). CWRES: conditional weighted residuals. Population (PRED) and individually (IPRED) predicted plasma concentrations of propofol and BIS (bispectral index) values were calculated using typical values and empirical Bayesian estimates of pharmacokinetic and pharmacodynamic parameters, respectively

External validation

A total of 599 plasma samples from 155 patients were available for measurement of plasma propofol concentrations, which were paired off with 301 BIS values from 78 patients for intermediate model and 286 BIS values from 77 patients for final model. Pooled biases, inaccuracies, divergences, and wobbles of the TCI systems of propofol are shown in Table 4. Pooled biases and inaccuracies in pharmacokinetic and pharmacodynamic predictions were clinically acceptable as described in earlier studies [30, 31]. Inclusion of mean infusion rate of remifentanil in the final pharmacodynamic model did not result in improvement of pharmacodynamic prediction, compared with the intermediate model. Plot of the measured to predicted concentration of propofol and BIS are presented. Prediction probability (SE, 95 % confidence interval) of propofol effect-site concentration was 0.7056 (0.0123, 0.6815–0.7297) for intermediate pharmacodynamics model and that was 0.7302 (0.0135, 0.7037–0.7567) for final pharmacodynamic model.

Simulations

The amounts of propofol given by intravenous boluses of propofol 3 mg kg^{-1} are 30 mg and 120 mg in children weighing 10 and 40 kg. These doses of propofol are diluted by the fixed value of V_1 estimate, resulting in lower initial plasma and effect-site propofol concentrations, hence, a higher predicted initial value of BIS in a 10 kg child, compared with those in a 40 kg child (Fig. 4, upper panel). The fixed value of V_1 estimate well described higher weight-based dose requirements of propofol in lighter children.

Plasma and effect-site concentrations of propofol during zero-order infusion of 200 μg kg^{-1} min^{-1} are higher in a 40 kg child, which, in turn, results in lower predicted BIS values. These simulation findings are attributed to a higher dose of propofol diluted in the fixed value of V_1 estimate in a heavier child. However, both the plasma and effect-site concentrations of propofol in a 40 kg child decrease more rapidly and eventually become lower than those in lighter children, leading to a more rapid recovery of predicted BIS

Table 4 Pooled biases (median performance error, MDPE), inaccuracies (median absolute performance error, MDAPE), divergences, and wobbles of the target effect-site concentration controlled infusion systems of propofol in pediatric patients

Parameter	Measured versus predicted propofol concentration (95 % CI)	Measured versus predicted BIS (95 % CI)	
		Intermediate model	Final model
Bias (%)	−20.21 (−23.31 to −18.12)	1.46 (−0.43 to 3.91)	−6.81 (−9.05 to −4.06)
Inaccuracy (%)	30.35 (28.62–32.72)	18.87 (17.34–20.54)	19.13 (17.46–20.85)
Divergence (% h^{-1})	19.14 (16.12–22.73)	−8.57 (−11.78 to −4.86)	−6.99 (−9.98 to −3.00)
Wobble (%)	11.48 (9.63–13.36)	8.50 (7.19–9.72)	9.97 (8.62–11.36)

The predicted value of BIS (bispectral index) was calculated using the following equations: Predicted BIS of intermediate model = $76.9 + (35.4 - 76.9)\frac{Ce^{3.02}}{(3.78-0.183\times \mathrm{age})^{3.02}+Ce^{3.02}}$, Predicted BIS of final model = $82.4 + (30.8 - 82.4)\frac{Ce^{2.1}}{(3.47-0.095\times \mathrm{age}-1.63\times \mathrm{REMI})^{2.1}+Ce^{2.1}}$, where *Ce* was effect-site concentration of propofol and REMI was mean infusion rate of remifentanil (μg kg^{-1} min^{-1})

values (Fig. 4, lower panel). These findings can be attributed to higher distributional and metabolic clearances with increasing weight.

Because pharmacokinetic parameters such as V_2 and metabolic clearance are determined based on weight only and the k_{e0} is a fixed value in this study, the simulated time courses of plasma and effect-site concentrations after administering weight-based doses of propofol are identical irrespective of age, as long as the body weight of each child is equal. Meanwhile, when weight-based dosing is employed, the younger (Fig. 5, left panel) or the lower mean infusion rate of remifentanil (Fig. 5, right panel), the higher predicted BIS values, because Ce_{50} increases with decreasing age and mean infusion rate of remifentanil. Context sensitive decrement time, which mainly influenced by metabolic clearance, was simulated to be shortened with increasing body weight (Fig. 6). In summary, the lighter (pharmacokinetically) and the younger (pharmacodynamically), the higher dose requirements of propofol in children.

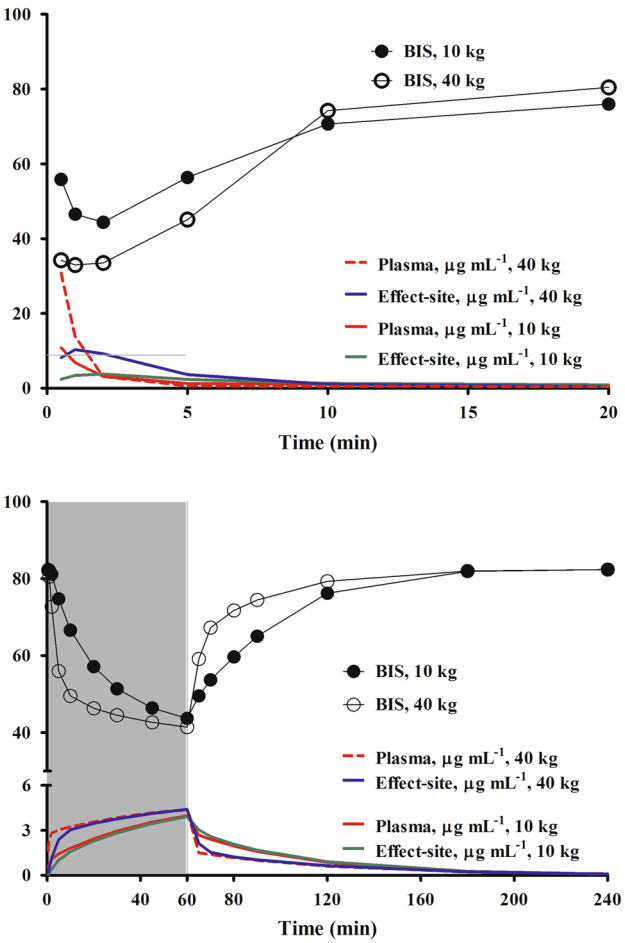

Fig. 4 Simulated time courses of plasma and effect-site concentrations of propofol, and bispectral index (BIS) values after administration of an intravenous bolus of 3 mg kg^{-1} (*upper panel*) and zero-order infusion at the rate of 200 μg kg^{-1} min^{-1} for 60 min (*lower panel*) in children weighing 10 or 40 kg. The age and mean remifentanil infusion rate throughout the operative period (bolus and infusion doses divided by the elapsed time from the first bolus to the end of infusion) were set at 8 years of age and 0.24 μg kg^{-1} min^{-1}, irrespective of body weight

Discussion and conclusions

In this study, we developed population pharmacokinetic and pharmacodynamic models of propofol in a single pediatric population, and performed an external validation using target-controlled infusion in a separate population of children.

Higher weight-based bolus dose requirements of propofol in lighter children

Clinically, the weight-based bolus dose of propofol for induction of anaesthesia should be increased by 50 % in children, compared with the adult dose [32]. Moreover, this

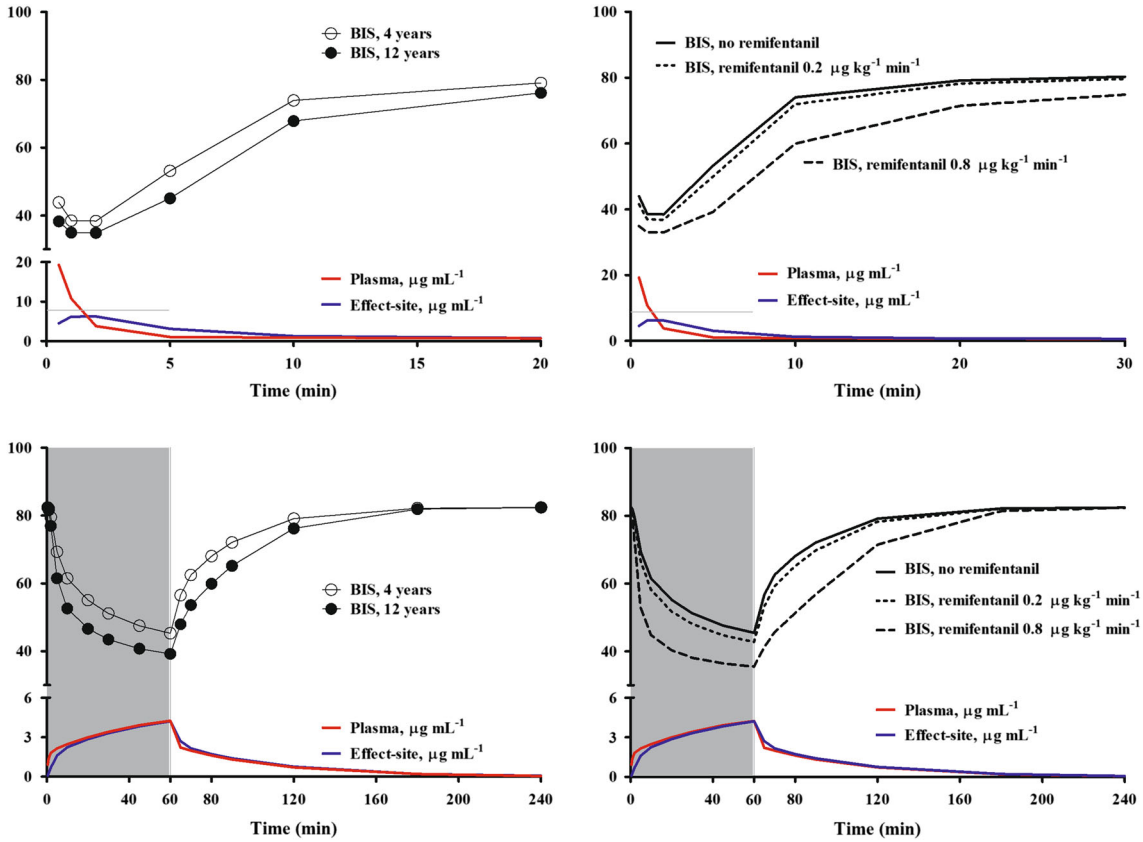

Fig. 5 Simulated time courses of the plasma and effect-site concentrations of propofol, and bispectral index (BIS) values after administration of an intravenous bolus of 3 mg kg^{-1} (*upper panels*) and zero-order infusion at the rate of 200 μg kg^{-1} min^{-1} for 60 min (*lower panels*). *Left panels* children aged 4 and 12 years. Body weight and mean infusion rate of remifentanil throughout the operative period were set at 20 kg and 0.24 μg kg^{-1} min^{-1}, irrespective of age. *Right panels* children receiving remifentanil at mean infusion rates of 0, 0.2, and 0.8 μg kg^{-1} min^{-1}. Body weight and age were set to 20 kg and 8 years, respectively

weight-based dose requirement in younger children (2 years of age) exceeded that required by older children (6–12 years of age) by 30.1 % [33]. The fixed value of the central volume of propofol in this study produces a higher volume per unit body weight with decreasing body weight. Lighter children, therefore, require a higher weight-based bolus dose to achieve a given initial concentration of propofol. Upon the same weight-based dose, simulated concentrations of propofol are lower in lighter children owing to smaller total dose of propofol. However, central volume of distribution in the Kataria model, which is linearly proportional to body weight, cannot describe higher bolus dose requirement of propofol in lighter children, because the same weight-based dose administered to children with different body weights should always result in the same initial plasma concentration [34]. On the other hand, Schüttler model, in which central volume of propofol is nonlinearly proportional to body weight, well describes lower plasma concentration in lighter children upon the same weight-based dose of propofol [3]. But this model does not provide a blood–brain equilibration rate constant (k_{e0}) essential to target effect-site concentration controlled infusion of propofol and has not been validated externally.

Higher weight-based infusion rate of propofol to maintain a level of concentration and prolonged context-sensitive half-time in lighter children

In this study, the lighter the children, the higher the weight-based infusion rate of propofol to maintain a certain level of plasma or effect-site concentration, as inferred in Fig. 4, lower panel. The integration of body weight to the metabolic clearance of propofol lead to substantial prolongations of the context-sensitive decrement times in children as body weight decreases (Fig. 6). These findings are in complete agreement with those of McFarlan et al. [35], and can be fully described using pharmacokinetic parameters, with which only body weight is associated, and the k_{e0} in this study. The major difference of the present study from that by McFarlan et al. is that the independent effects of body weight (pharmacokinetically) and age (pharmacodynamically) on the infusion rate of propofol

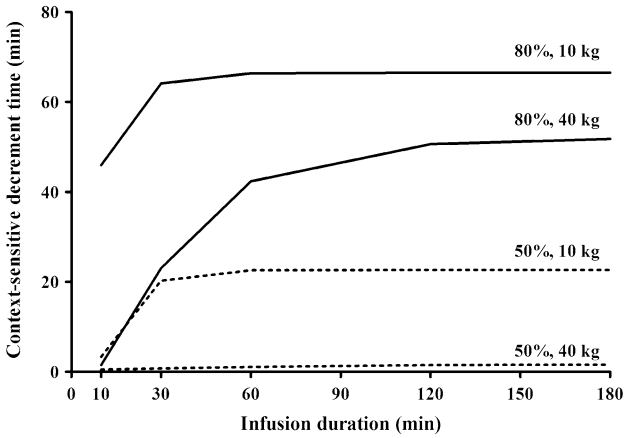

Fig. 6 Context-sensitive decrement times for 50 and 80 % decreases in plasma propofol concentration after target plasma concentration-controlled infusion for varying durations in children weighing at 10 and 40 kg

required to produce a given level of plasma or effect-site concentration were delineated.

Higher weight-based infusion rate of propofol to maintain a given level of BIS in younger children

The infusion rate of propofol to maintain any designated BIS level (which measures the response to propofol) depends on both body weight and age in the children population, as inferred in Figs. 4, lower panel and 5, left lower panel. The relationships between BIS and the effect-site concentration of propofol shown in Eq. 1 exemplify this assertion. The effect-site concentration needed to produce a particular BIS level can be calculated using pharmacodynamic parameters such as E_0, E_{max}, γ, and Ce_{50}. Age is involved in this calculation as a covariate of Ce_{50}. Then, k_{e0} and pharmacokinetic parameters are required to calculate the propofol dose requirement to maintain the calculated effect-site concentration corresponding to that level of BIS. Notably, calculated effect-site concentration of propofol to produce a given value of BIS varied not by body weight, but by age and the mean infusion rate of remifentanil, because body weight is not involved in calculation of the effect-site concentration in Eq. 1. Many earlier studies reported increased sensitivity to propofol in children using pharmacodynamic analysis only [1, 5, 36]. However, when pharmacokinetic parameters derived from separate pharmacokinetic studies are used for pharmacodynamic modeling, the individual effects of pharmacokinetic and pharmacodynamic characteristics in terms of the higher propofol dose requirements in the children population cannot be evaluated accurately and precisely.

Remifentanil reduces the weight-based dose requirements of propofol

Several studies have also shown that opioids dramatically reduce the concentrations of propofol required for achievement of various clinical and electroencephalographic endpoints [37, 38]. Response surface modeling has been used to evaluate potential drug interactions between the two drugs with common clinical responses, at the entire ranges of their concentrations [39]. However, complex dosing schemes and relatively long time for achieving pseudo-steady states of drug concentrations for certain levels of response make response surface methodology less available in clinical settings. Instead, we decided to include the total dose of remifentanil from induction to the end of anaesthesia in the form of mean infusion rates which is more easily understandable to the clinical practitioners. Of course, we also sought to include the bolus dose and instantaneous infusion rates of remifentanil as time-varying covariates, but we failed to successfully fit the data. In simulation studies, the effect of remifentanil on the propofol dose requirement was almost twice those of age and body weight. This simulation is supported by an earlier study that demonstrated a synergistic interaction between propofol and remifentanil for maintenance of a BIS value between 45 and 55 [12].

Which model is better to titrate propofol during anaesthesia in children?

A TCI system, which is well known as a method to maintain a nominal target concentration, can induce and maintain target concentration of propofol using a pharmacokinetic model. The pharmacokinetic parameters and k_{e0} including covariates are programmed into a TCI system, without considering the inter- and intra-individual variability. The effect-site concentration-controlled infusion of propofol is a more effective method to titrate surgical stresses during anesthesia than manual infusion, because effect-site concentration determines the effect of a drug. Although predicted BIS values in the final pharmacodynamic model may be more reliable than those in the intermediate model, mean infusion rate of remifentanil in Eq. 12 is unobtainable during clinical practice and hence, the final pharmacodynamic model is not applicable to predicting BIS in real-time. Predicted BIS values in the intermediate pharmacodynamic model reflect at least age and body weight dependent dose alterations of propofol, and can be obtained in real time during anaesthesia. Also, model performances of the two models were comparable each other. Hence, we thought that the intermediate pharmacodynamic model may be reliably applicable to target

effect-site concentration controlled infusion in clinical practice.

Comparison of sampling scheme with Kataria model

Pharmacokinetics of propofol in children has been described by three compartment mammillary models [3, 34, 40–43]. Of these models, sampling schedule was described only in Kataria model [34]. Arterial blood was used for model building in this study, while venous blood, in Kataria model. Both studies were conducted with an intravenous bolus and subsequent variable rate infusion. Initial sampling time after an intravenous bolus of propofol in Kataria model was 1.5 min, while 2 min in this study. The two studies are not substantially different in terms of sampling scheme. Time course of plasma concentration of propofol in children was well described by two compartment mammillary model in this study, which was partly explained by the relatively late initial sampling time and early last sampling time after discontinuation of propofol infusion. This point was a limitation of this study due to sampling difficulties, especially at the beginning of administration of bolus dose and at late postinfusion times. It is needed to check the potential error for longer infusions using this model in a TCI system.

Midazolam and remifentanil

In this study, midazolam was given before induction, and all children were lightly sedated, as indicated by the average baseline BIS of 82.2 ± 7.0. In general, this is a usual clinical practice, on which pharmacokinetic and pharmacodynamic modeling of propofol should be based. Because all patients received the same weight-based dose of midazolam, additional inter-individual variability imposed on pharmacodynamic parameters by the administration of midazolam might not be substantial, as indicated by the small coefficient of variation of the baseline BIS value (8.5 %). In an earlier study to evaluate triple pharmacodynamic interactions involving intravenous bolus doses of midazolam, propofol and alfentanil, there was no triple synergy of all three drugs beyond the synergy of all paired drugs [39]. Moreover, external validation demonstrated that predictive performances in pharmacodynamic predictions in this study were much better than those in pharmacokinetic predictions. We, therefore, thought that midazolam probably has minimal influence on the estimate of k_{e0}, which was the important parameter carried forward to the TCI system.

Although remifentanil does not alter the pharmacokinetics of propofol, propofol increases the initial remifentanil concentration after a bolus but minimally increases the concentrations during maintenance phase [44]. Because we did not measure blood concentrations of remifentanil, possible increase of remifentanil concentrations during induction phase and resultant influence on observed BIS values were not evaluated. However, we consider that any such effect may be minimal because bolus doses of remifentanil during induction were 1 μg kg^{-1} in all patients and remifentanil changes processed electroencephalograms at very high concentrations [45]. Although inter-individual variability of k_{e0} increased after inclusion of age and remifentanil in the pharmacodynamic models in this study, all the estimates of pharmacodynamic parameters were statistically sound, as indicated by relative standard errors less than 50 % and narrow 95 % confidence intervals. The final value for k_{e0} in this study equates to an equilibrium half-life of 1.87 min. This is more rapid than values for adults (5.68 and 5.13 min for man) [46, 47]. This phenomenon may be explained by some facts. First, fraction of the cardiac output distributed to the vessel-rich organ including brain is generally greater in children than in adults [48]. Second, immaturity of the blood–brain barrier can lead to higher brain concentrations of lipophilic drug [49].

External validation

Pooled biases and inaccuracies in pharmacokinetic predictions of propofol were clinically acceptable in this study (bias: <10–20 % and inaccuracy: approximately 20–30 %) [30, 31, 50], while those of Kataria and Schnider models failed to meet these criteria [1]. The reason for showing overestimation of plasma concentration of propofol in this study may be found in three aspects. First, during target controlled infusion, pharmacokinetic parameters derived from administration of bolus dose showed worse prediction than those derived from infusion data [51]. Second, it seems that allometric scaling well described the age-related changes of metabolic clearance in children than linear weight-clearance relationship [52]. The almost linear weight-clearance relationship was observed in this pharmacokinetic model. Third, relatively low number of early samples after administration of bolus dose may influenced the estimation of pharmacokinetic parameters, especially volume of distribution of central compartment (V1). The value of V1 in this study was relatively lower than those of other pediatric pharmacokinetic models (the range of V1: 1.74–10.3 for a 10 kg 1-year-old patient) [53]. Divergence, an index of how the resulting drug concentrations in a patient are affected by time, was slightly high, compared with those in adults (−2 to 13.2 % h^{-1}) [30]. In general, divergence is best determined by maintaining a single target concentration over time. We employed stepwise increases in target concentration of propofol followed by stepwise decreases, which might worsen divergence.

Moreover, to our knowledge, there has been no study to evaluate divergence of a pharmacokinetic model of propofol in children. Comparison of predictive performances for pharmacokinetic models of propofol are shown [1, 30].

Conclusion

The altered weight-based dose requirements of propofol (bolus dose and infusion rate) are well described pharmacokinetically (as a fixed volume of central compartment and the inclusion of body weight in V_2 and metabolic clearance), and pharmacodynamically (the effects of age and remifentanil on the potency). The lighter the child, the higher weight-based requirements in bolus dose and infusion rate of propofol to achieve a given plasma or effect-site concentration. The younger the child and the lower the mean infusion rate of remifentanil, the higher weight-based dose requirements of propofol (bolus and infusion) to produce a given level of BIS. Predictive performances of target controlled infusion system incorporating pharmacokinetic parameters and k_{e0} in this study were clinically acceptable.

Acknowledgments We are grateful to In-Jin Jang, M.D. and Kyung-Sang Yu, M.D. from the Clinical Research Center of Seoul National University (Seoul, Korea) for measuring plasma concentrations of propofol. This work was supported by the Seoul National University Hospital Research Fund (0420100190, 0420110910) of Seoul National University Hospital and the Student Research Grant (11-12) of University of Ulsan College of Medicine, Seoul, Korea.

References

1. Rigouzzo A, Servin F, Constant I (2010) Pharmacokinetic-pharmacodynamic modeling of propofol in children. Anesthesiology 113:343–352
2. Cote CJ (2010) Pediatric anesthesia. In: Miller RD (ed) Miller's anesthesia, 7th edn. Churchill Livingstone, an imprint of Elsevier Inc., Philadelphia, pp 2559–2597
3. Schuttler J, Ihmsen H (2000) Population pharmacokinetics of propofol: a multicenter study. Anesthesiology 92:727–738
4. Murat I, Billard V, Vernois J, Zaouter M, Marsol P, Souron R, Farinotti R (1996) Pharmacokinetics of propofol after a single dose in children aged 1–3 years with minor burns. Comparison of three data analysis approaches. Anesthesiology 84:526–532
5. Hammer GB, Litalien C, Wellis V, Drover DR (2001) Determination of the median effective concentration (EC50) of propofol during oesophagogastroduodenoscopy in children. Paediatr Anaesth 11:549–553
6. Rigouzzo A, Girault L, Louvet N, Servin F, De-Smet T, Piat V, Seeman R, Murat I, Constant I (2008) The relationship between bispectral index and propofol during target-controlled infusion anesthesia: a comparative study between children and young adults. Anesth Analg 106:1109–1116
7. Suggs DM (2000) Pharmacokinetics in children: history, considerations, and applications. J Am Acad Nurse Pract 12:236–239
8. Constant I, Rigouzzo A (2010) Which model for propofol TCI in children. Paediatr Anaesth 20:233–239
9. Blusse van Oud-Alblas HJ, Peters JW, de Leeuw TG, Tibboel D, Klein J, Weber F (2008) Comparison of bispectral index and composite auditory evoked potential index for monitoring depth of hypnosis in children. Anesthesiology 108:851–857
10. Lysakowski C, Dumont L, Pellegrini M, Clergue F, Tassonyi E (2001) Effects of fentanyl, alfentanil, remifentanil and sufentanil on loss of consciousness and bispectral index during propofol induction of anaesthesia. Br J Anaesth 86:523–527
11. Fechner J, Hering W, Ihmsen H, Palmaers T, Schuttler J, Albrecht S (2003) Modelling the pharmacodynamic interaction between remifentanil and propofol by EEG-controlled dosing. Eur J Anaesthesiol 20:373–379
12. Ropcke H, Konen-Bergmann M, Cuhls M, Bouillon T, Hoeft A (2001) Propofol and remifentanil pharmacodynamic interaction during orthopedic surgical procedures as measured by effects on bispectral index. J Clin Anesth 13:198–207
13. Kern SE, Xie G, White JL, Egan TD (2004) A response surface analysis of propofol-remifentanil pharmacodynamic interaction in volunteers. Anesthesiology 100:1373–1381
14. Beal S, Sheiner L (1992) NONMEM user's guides. In: Part V introductory guide. NONMEM Project Group, University of California, San Francisco, p 48
15. Mosteller RD (1987) Simplified calculation of body-surface area. N Engl J Med 317:1098
16. Hallynck TH, Soep HH, Thomis JA, Boelaert J, Daneels R, Dettli L (1981) Should clearance be normalised to body surface or to lean body mass? Br J Clin Pharmacol 11:523–526
17. Deurenberg P, Weststrate JA, Seidell JC (1991) Body mass index as a measure of body fatness: age- and sex-specific prediction formulas. Br J Nutr 65:105–114
18. Janmahasatian S, Duffull SB, Ash S, Ward LC, Byrne NM, Green B (2005) Quantification of lean bodyweight. Clin Pharmacokinet 44:1051–1065
19. Schwartz GJ, Haycock GB, Edelmann CM Jr, Spitzer A (1976) A simple estimate of glomerular filtration rate in children derived from body length and plasma creatinine. Pediatrics 58:259–263
20. Lee SH, Ghim JL, Song MH, Choi HG, Choi BM, Lee HM, Lee EK, Roh YJ, Noh GJ (2009) Pharmacokinetics and pharmacodynamics of a new reformulated microemulsion and the long-chain triglyceride emulsion of propofol in beagle dogs. Br J Pharmacol 158:1982–1995
21. Schnider TW, Minto CF, Gambus PL, Andresen C, Goodale DB, Shafer SL, Youngs EJ (1998) The influence of method of administration and covariates on the pharmacokinetics of propofol in adult volunteers. Anesthesiology 88:1170–1182
22. Bartkowska-Sniatkowska A, Bienert A, Wiczling P, Owczarek M, Rosada-Kurasinska J, Grzeskowiak M, Matysiak J, Kokot ZJ, Kaliszan R, Grzeskowiak E (2014) Pharmacokinetics and pharmacodynamics of propofol in children undergoing different types of surgeries. Pharmacol Rep 66:821–829
23. Bjornsson MA, Norberg A, Kalman S, Karlsson MO, Simonsson US (2010) A two-compartment effect site model describes the bispectral index after different rates of propofol infusion. J Pharmacokinet Pharmacodyn 37:243–255
24. Wahlby U, Jonsson EN, Karlsson MO (2001) Assessment of actual significance levels for covariate effects in NONMEM. J Pharmacokinet Pharmacodyn 28:231–252
25. Parke J, Holford NH, Charles BG (1999) A procedure for generating bootstrap samples for the validation of nonlinear mixed-effects population models. Comput Methods Programs Biomed 59:19–29

26. Karlsson MO, Savic RM (2007) Diagnosing model diagnostics. Clin Pharmacol Ther 82:17–20
27. Bergstrand M, Hooker AC, Wallin JE, Karlsson MO (2011) Prediction-corrected visual predictive checks for diagnosing nonlinear mixed-effects models. AAPS J 13:143–151
28. Varvel JR, Donoho DL, Shafer SL (1992) Measuring the predictive performance of computer-controlled infusion pumps. J Pharmacokinet Biopharm 20:63–94
29. Smith WD, Dutton RC, Smith NT (1996) Measuring the performance of anesthetic depth indicators. Anesthesiology 84:38–51
30. Glen JB, Servin F (2009) Evaluation of the predictive performance of four pharmacokinetic models for propofol. Br J Anaesth 102:626–632
31. Glass PA, Shafer SL, Reves JG (2009) Intravenous drug delivery systems. In: Miller RD (ed) Intravenous drug delivery systems, 7th edn. Churchill Livingstone, Philadelphia, pp 825–858
32. Smith I, White PF, Nathanson M, Gouldson R (1994) Propofol. An update on its clinical use. Anesthesiology 81:1005–1043
33. Aun CS, Short SM, Leung DH, Oh TE (1992) Induction dose-response of propofol in unpremeditated children. Br J Anaesth 68:64–67
34. Kataria BK, Ved SA, Nicodemus HF, Hoy GR, Lea D, Dubois MY, Mandema JW, Shafer SL (1994) The pharmacokinetics of propofol in children using three different data analysis approaches. Anesthesiology 80:104–122
35. McFarlan CS, Anderson BJ, Short TG (1999) The use of propofol infusions in paediatric anaesthesia: a practical guide. Paediatr Anaesth 9:209–216
36. Hahn JO, Khosravi S, Dumont GA, Ansermino JM (2011) Two-stage vs mixed-effect approach to pharmacodynamic modeling of propofol in children using state entropy. Paediatr Anaesth 21:691–698. doi:10.1111/j.1460-9592.2011.03584.x
37. Bouillon TW, Bruhn J, Radulescu L, Andresen C, Shafer TJ, Cohane C, Shafer SL (2004) Pharmacodynamic interaction between propofol and remifentanil regarding hypnosis, tolerance of laryngoscopy, bispectral index, and electroencephalographic approximate entropy. Anesthesiology 100:1353–1372
38. Milne SE, Kenny GN, Schraag S (2003) Propofol sparing effect of remifentanil using closed-loop anaesthesia. Br J Anaesth 90:623–629
39. Minto CF, Schnider TW, Short TG, Gregg KM, Gentilini A, Shafer SL (2000) Response surface model for anesthetic drug interactions. Anesthesiology 92:1603–1616
40. Absalom A, Amutike D, Lal A, White M, Kenny GN (2003) Accuracy of the 'Paedfusor' in children undergoing cardiac surgery or catheterization. Br J Anaesth 91:507–513
41. Absalom A, Kenny G (2005) 'Paedfusor' pharmacokinetic data set. Br J Anaesth 95:110
42. Marsh B, White M, Morton N, Kenny GN (1991) Pharmacokinetic model driven infusion of propofol in children. Br J Anaesth 67:41–48
43. Short TG, Aun CS, Tan P, Wong J, Tam YH, Oh TE (1994) A prospective evaluation of pharmacokinetic model controlled infusion of propofol in paediatric patients. Br J Anaesth 72:302–306
44. Bouillon T, Bruhn J, Radu-Radulescu L, Bertaccini E, Park S, Shafer S (2002) Non-steady state analysis of the pharmacokinetic interaction between propofol and remifentanil. Anesthesiology 97:1350–1362
45. Noh GJ, Kim KM, Jeong YB, Jeong SW, Yoon HS, Jeong SM, Kang SH, Linares O, Kern SE (2006) Electroencephalographic approximate entropy changes in healthy volunteers during remifentanil infusion. Anesthesiology 104:921–932
46. Jung JA, Choi BM, Cho SH, Choe SM, Ghim JL, Lee HM, Roh YJ, Noh GJ (2010) Effectiveness, safety, and pharmacokinetic and pharmacodynamic characteristics of microemulsion propofol in patients undergoing elective surgery under total intravenous anaesthesia. Br J Anaesth 104:563–576
47. Kim KM, Choi BM, Park SW, Lee SH, Christensen LV, Zhou J, Yoo BH, Shin HW, Bae KS, Kern SE, Kang SH, Noh GJ (2007) Pharmacokinetics and pharmacodynamics of propofol microemulsion and lipid emulsion after an intravenous bolus and variable rate infusion. Anesthesiology 106:924–934
48. Anderson BJ (2011) An introduction to the intricacies of pharmacology in pediatrics. In: Bissonnette B (ed) Pediatric anesthesia. People's Medical Publishing House, Shelton, pp 291–293
49. Lipscomb JC, Ohanian EV (2006) Toxicokinetics and risk assessment. Informa Healthcare, New York, pp 231–249
50. Schuttler J, Kloos S, Schwilden H, Stoeckel H (1988) Total intravenous anaesthesia with propofol and alfentanil by computer-assisted infusion. Anaesthesia 43(Suppl):2–7
51. Vuyk J, Engbers FH, Burm AG, Vletter AA, Bovill JG (1995) Performance of computer-controlled infusion of propofol: an evaluation of five pharmacokinetic parameter sets. Anesth Analg 81:1275–1282
52. Anderson BJ, Holford NH (2011) Tips and traps analyzing pediatric PK data. Paediatr Anaesth 21:222–237. doi:10.1111/j.1460-9592.2011.03536.x
53. Sepulveda P, Cortinez LI, Saez C, Penna A, Solari S, Guerra I, Absalom AR (2011) Performance evaluation of paediatric propofol pharmacokinetic models in healthy young children. Br J Anaesth 107:593–600. doi:10.1093/bja/aer198